

Cite this: *RSC Sustainability*, 2024, 2, 616Received 19th September 2023  
Accepted 6th January 2024

DOI: 10.1039/d3su00330b

rsc.li/rscsus

# Sustainable artificial coral reef restoration using nanoclays and composite hydrogel microcapsules†

Mohammad Fahimizadeh,<sup>ab</sup> Febriane Sukiato,<sup>c</sup> Kok Lynn Chew,<sup>cd</sup>  
Yang Amri Affendi,<sup>c</sup> Pooria Pasbakhsh,<sup>ab\*</sup> Joash Ban Lee Tan,<sup>ef</sup>  
R. K. Singh Raman<sup>g</sup> and Peng Yuan<sup>b</sup>

This report assesses the potential of sustainably-produced artificial coral reef materials metakaolin clay, hydrogel microcapsules, and nanocomposite microcapsule-encapsulated calcifying bacteria as artificial coral reef constituents. The findings show that nanoclays and hydrogels can be considered safe, potential artificial reef constituents, and can improve the sustainability of artificial reefs.

Coral reefs are mostly composed of hard corals with skeletons made of calcium carbonate. They are found in shallow waters of tropical and subtropical oceans worldwide, providing habitats for various marine organisms.<sup>1,2</sup> The Coral Triangle is an area with the highest marine biodiversity in the world,<sup>3</sup> and Malaysia is one of the countries located in this area. It is estimated that Malaysia contains 1595.21 km<sup>2</sup> of coral reefs and gains multiple environmental and economic benefits from its coral reefs.<sup>4,5</sup> The Department of Marine Park Malaysia evaluated that its marine protected areas with coral reefs generated approximately USD 1.93 billion in total economic value from its ecosystem services from 2011 to 2015.<sup>6</sup>

In recent decades, global coral reef cover has declined due to anthropogenic factors such as pollution, unsustainable coastal development, and destructive fishing practices.<sup>7,8</sup> However, climate change brought about by global warming has been

## Sustainability spotlight

In July 2023, the global ocean surface temperatures reached unprecedented levels due to anthropogenic global warming. Current projections for the coming decades spell doom for marine organisms not adapted to survive in warmer and more acidic seas. Among the most vulnerable are coral reefs, which form the backbone of numerous marine ecosystems. Coral reefs are under tremendous pressure from global warming, disease outbreaks, and pollution, losing substantial coverage every year. This short communication describes an interdisciplinary effort to assess the potential of novel, environmentally sustainable construction additives for coral reef restoration. The findings can lead to the construction of better performing and more sustainable artificial reefs, coastal and offshore structures, and coral nursery materials, firmly aligning the progress of the field with several United Nations Sustainable Development Goals (SDGs), namely SDG9 (Industry, Innovation and Infrastructure), SDG13 (Climate Action), and SDG 14 (Life Below Water), to address and mitigate the threats posed by global warming.

identified as the main cause of the decline of coral reefs worldwide,<sup>8,9</sup> and various coral restoration efforts have been taken to assist in the recovery of degraded reefs.<sup>10</sup> According to a recent coral restoration review, 21% of coral restoration projects worldwide deploy artificial reef structures to increase habitat for marine life and fisheries production of coral reefs, provide coastal recreational activities (*i.e.*, SCUBA diving), and prevent destructive fishing activities.<sup>2</sup> In Malaysia, artificial reef structures have been deployed since 1975 to conserve marine areas by preventing trawling activities in nearshore areas, providing habitat for marine life, and boosting commercial fish populations to improve the catches of artisanal fishermen.<sup>11,12</sup> Another notable use of artificial reef structure is to provide an area for coral larvae to settle and thrive.<sup>13</sup> Mobile coral larvae depend on physical cues to determine their settlement location and often seek deposits of crustose coralline algae (CCA) with a rugose-textured surface.<sup>14</sup> Moreover, an *in situ* study by Gorceau<sup>15</sup> found that increased calcium carbonate formation can stimulate the settlement of coral larvae, growth of coral, and other calcifying organisms. The importance of the presence of

<sup>a</sup>School of Engineering, Monash University Malaysia, Jalan Lagoon Selatan, 47500 Bandar Sunway, Selangor, Malaysia. E-mail: Pooria.pasbakhsh@monash.edu

<sup>b</sup>School of Environmental Science and Engineering, Guangdong University of Technology, Guangzhou, 510006, China

<sup>c</sup>Institute of Ocean and Earth Sciences (IOES), Universiti Malaya, 50603 Kuala Lumpur, Wilayah, Kuala Lumpur, Malaysia

<sup>d</sup>Coralku Solutions, 6000 Kuala Lumpur, 6000 Wilayah Kuala Lumpur, Malaysia

<sup>e</sup>School of Science, Monash University Malaysia, Jalan Lagoon Selatan, 47500 Bandar Sunway, Selangor, Malaysia

<sup>f</sup>Tropical Medicine and Biology Multidisciplinary Platform, Monash University Malaysia, Jalan Lagoon Selatan, 47500 Bandar Sunway, Selangor, Malaysia

<sup>g</sup>Department of Chemical and Biological Engineering, Department of Mechanical and Aerospace Engineering, Monash University, Clayton 3168, Australia

† Electronic supplementary information (ESI) available. See DOI: <https://doi.org/10.1039/d3su00330b>



calcium carbonate for coral attachment has been highlighted in other studies.<sup>16,17</sup>

Artificial reef structures are commonly fabricated using standard construction materials, such as cement and steel bars. Such materials are widely available and have predictable performance and service life. However, cement and steel production has a high environmental impact.<sup>18,19</sup> The durability of steel-reinforced cement-based structures is significantly lowered by crack formation and ingress of corrosive elements such as chloride, which makes the artificial reef material susceptible to strong waves and surges, lowering the service life of the artificial reef material.<sup>20</sup> Considering the intensifying pressure on coral reef ecosystems and cement-based structures due to global warming and ocean acidification, artificial coral reefs are candidates for multidisciplinary research. Self-healing of concrete is a novel and sustainable technique that can autonomously fix structural concrete cracks and fill small pores, extending the service life of concrete structures.<sup>18</sup> Concrete self-healing systems rely on chemical and biological healing agents, of which the biological pathway is considered the most sustainable. Biological concrete self-healing relies on calcium carbonate precipitation by alkaliphilic spore-forming bacteria that can withstand the harsh cement environment. Calcium carbonate precipitation is triggered only after structural faults introduce water and oxygen into the cement matrix, resulting in spore germination.

When the self-healing system is concentrated on the structure's outer surface, this trigger is no longer needed to initiate biomineralization as the bacterial spores would readily germinate. Bacterial self-healing concrete systems can also increase calcium-silicate-hydrate (CSH) gel formation in concrete.<sup>18</sup> Alongside the increased calcium carbonate formation, this aspect can improve concrete's structural resistance and surface complexity.

Biological healing agents are susceptible to the harsh alkaline cement environment and therefore require protection, often provided by solid carriers such as expanded clay,<sup>21</sup> nanoclay,<sup>22</sup> lightweight aggregate,<sup>23</sup> and hydrogels such as calcium alginate (CaAlg) microcapsules.<sup>24,25</sup> Alginate is harvested from brown algae and readily cross-links into a biopolymer with divalent cations such as calcium ions. As a hydrogel, CaAlg can store water beneficial for biological activity and cement hydration through internal curing. Also, cross-linked CaAlg capsules possess a complex surface that may benefit coral settlement and attachment. However, CaAlg can degrade due to the high alkalinity of the cement environment,<sup>24</sup> and can benefit from structural reinforcement by additives such as halloysite clay nanoparticles (HNT).<sup>26,27</sup> HNTs can further add to the surface complexity of CaAlg microcapsules and improve coral attachment while strengthening the cement matrix and CaAlg-cement bonding through pozzolanic reactions.<sup>28–30</sup> Other pozzolans, like metakaolin, can also benefit coral attachment by providing complex surfaces and pozzolanic reactions that improve the cement matrix.<sup>31,32</sup> Another interesting aspect is the potential of CaAlg to be colonized by beneficial reef microorganisms that can help sustain a healthy reef.<sup>33</sup>

In the current report, the impact of metakaolin (MK) and various microcapsules added to cement paste samples on the health and attachment of coral fragments and the structure of the cement paste samples were investigated. The summary of the samples is presented in Table 1. A full description of the cement paste samples preparation and constituents has been provided in ESI Appendix A, Table SI2.† Adding metakaolin to the cement paste resulted in a loss of structural order in metakaolin. The metakaolin in-plane Si–O–Si stretching band at 1035 cm<sup>-1</sup> disappeared after cement paste incorporation (Fig. 1b). The band at 3620 cm<sup>-1</sup> is attributed to the stretching vibration of the inner –OH groups, and the bands at 3696 cm<sup>-1</sup>, 3669 cm<sup>-1</sup> and 3656 cm<sup>-1</sup>, that are attributed to the stretching of inner octahedral surface –OH groups all experienced intensity loss, and peak broadening (Fig. 1a). This observation has been previously considered as a sign of geopolymerization.<sup>34</sup>

The intensity of the bands attributed to CaCO<sub>3</sub> increased after the addition of metakaolin to the cement paste; however, the relative intensity of 873 cm<sup>-1</sup> was lowered while the relative intensity of 855 cm<sup>-1</sup> increased in metakaolin-containing cement paste samples, indicating higher vaterite content relative to calcite (Fig. 1c).<sup>24,35</sup> Comparison of the relative intensities of the 873 cm<sup>-1</sup> and 855 cm<sup>-1</sup> peaks suggests a higher calcite proportion in T2, T3, T4, and T5 samples than in cement paste control samples (Fig. 1c).

FTIR spectra of microcapsules separated from cement paste samples after nine weeks of artificial seawater exposure displayed evidence of CaCO<sub>3</sub> formation in all microcapsules, with greater intensity of the corresponding peak for the ASHY microcapsules. Furthermore, Ca-alginate de-crosslinking is evidenced by shifts in 1575 cm<sup>-1</sup> and 1418 cm<sup>-1</sup> peaks towards wavenumbers associated with Na-alginate for all microcapsules (Fig. 2b). The trend in peak shift suggests that AH microcapsules display the highest resistance to de-crosslinking than other microcapsules. The likely reason behind Ca-alginate de-crosslinking is the substitution of Ca<sup>2+</sup> with Na<sup>+</sup> and Mg<sup>2+</sup> (Fig. 2c). The presence of HNTs in the AH microcapsules seems to decrease the rate of dissociation of Ca<sup>2+</sup> from the Ca-alginate polymer chains, hypothetically by carrying forward Ca<sup>2+</sup> ions from the Ca<sup>2+</sup>-alginate crosslinking step of the microcapsule preparation process, into the cement-embedded microcapsules (Fig. 2c). The presence of an intense band at 3692 cm<sup>-1</sup> in the spectra of CaAlg and ASHY microcapsules can be attributed to

**Table 1** Description of sample series and the elements present in each treatment, wherein MK denotes metakaolin, Alg denotes sodium alginate, HNT denotes halloysite nanotubes, YE denotes yeast extract, and S denotes bacterial spores

Cement paste series	Capsule type	Elements				
		MK	Alg	HNT	YE	S
C	–	–	–	–	–	–
T1	–	+	–	–	–	–
T2	CaAlg	+	+	–	–	–
T3	AH	+	+	+	–	–
T4	ASHY	+	+	+	+	+
T5	ASY	+	+	–	+	+



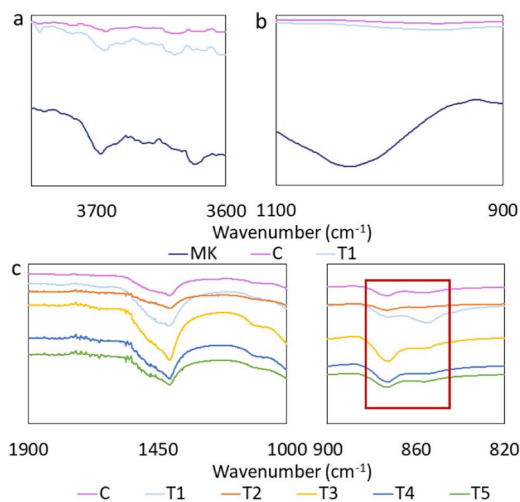


Fig. 1 FTIR spectra of (a and b) the matrix of C and T1 samples after nine weeks of artificial seawater (ASW) exposure and pristine meta-kaolin, and (c) the matrix of all cement paste types after nine weeks of ASW exposure with  $\text{CaCO}_3$  peaks highlighted in the red rectangle.

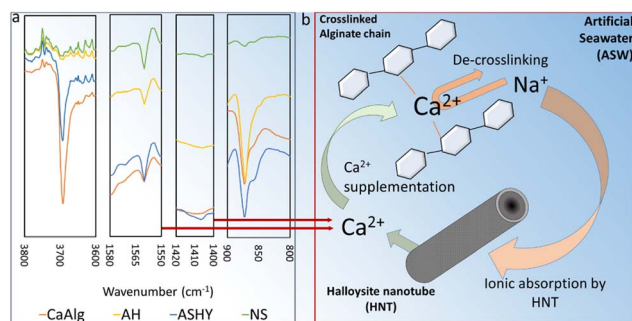


Fig. 2 (a) FTIR spectra of different microcapsules removed from cement paste samples after nine weeks of ASW exposure, (b) the possible interplay between ASW, HNTs, crosslinked  $\text{Ca}^{2+}$ , environmental ions (e.g.,  $\text{Na}^+$ ) and CaAlg chains.

non-structural  $-\text{OH}$  (Fig. 2a),<sup>36</sup> which also indicates the presence of Na or Ca hydroxides in the CaAlg and AH microcapsules.

No significant differences were detected in coral color scores between treatments throughout the experiment between

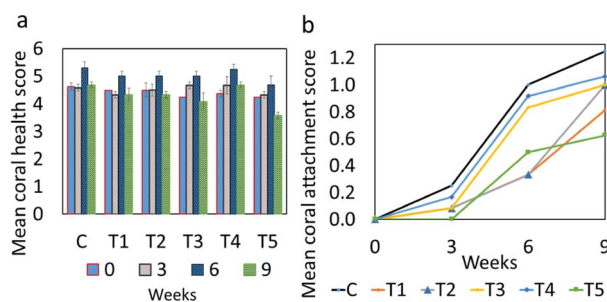


Fig. 3 Nine-week measurements of mean coral (a) health score and (b) attachment score. The error bars for health score measurements are based on standard deviation.

treatments or across different weeks (Fig. 3, statistics in ESI Appendix B†). The highest coral health scores observed were from coral fragments attached to C and T4 cement paste samples, reaching the approximate mean health score of 5.3 after six weeks. Coral fragments attached to different cement paste samples recovered to varying degrees from the stress of sampling and transplantation. The assessment-wide drop in the health scores at week nine occurred possibly due to an increase in water and atmospheric temperatures caused by a local heatwave. Such stresses were experienced by all coral fragments, and all fragments had recovered from the initial stress prior to the experiment. The stresses and recovery were judged based on significant colour changes, visible signs of stress post fragmentation, transportation and during treatment.

The coral health score findings confirm that the elements in the artificial reef samples, *i.e.*, the cement, meta-kaolin, calcium alginate, halloysite nanotubes, the bacteria, and the nutrients, may have no adverse effects on coral health.

It should be noted that among all components, only the bacteria, the nutrients, and minute quantities of calcium ions or calcium lactate leftover from the capsule formation steps would diffuse into the aqueous phase. No sudden changes in water parameters were observed during the initial days of placing the cement paste samples into the closed aquarium systems despite the expected diffusion of constituents, such as  $\text{Ca}(\text{OH})_2$  and  $\text{Ca}^{2+}$ . Therefore, the constituents of the cement paste samples can be considered safe for coral attachment.

Coral attachment to different cement paste samples was visually evident after three weeks (Fig. 3 and 4). Coral fragments in all treatments gradually initiated the attachment process, as evident from the formation of soft tissue in the fragment-cement paste interface (Fig. 4). The retraction of this new

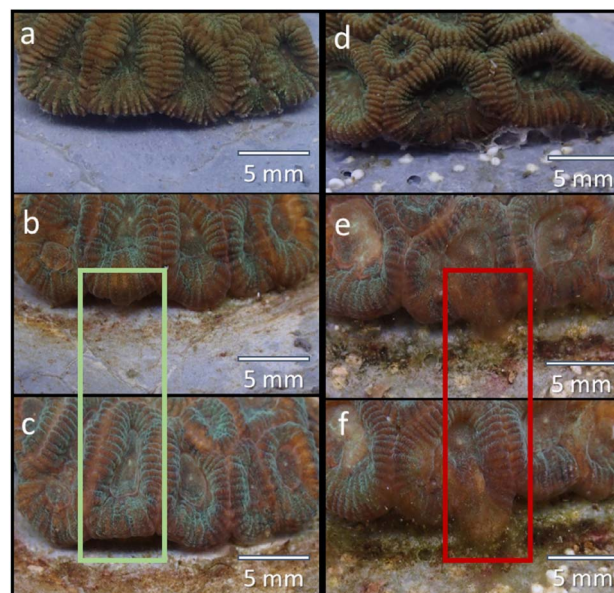


Fig. 4 Photographs of the attachment sites of different corals on Day 1, Day 46, and Day 66 in descending order; (a–c, black box) C corals, (d–f, blue box) T3 corals. The green and red boxes highlight areas of tissue growth.



tissue formation was also observed in some fragments (Fig. 4b and c). Overall, no significant differences were detected in attachment scores between treatments on any day of the experiment (Fig. 3 and 4, statistics in ESI Appendix C†). Coral attachment first became noticeable in control samples after 18 days, and all fragments initiated attachment after 36 days. This finding suggests that the microcapsules did not negatively impact coral attachment. The findings infer that the coral attachment was not affected by the increase in the surface complexity brought upon by the inclusion of the microcapsules, as well as the presence of varying textures, surface charges, and active chemical groups on the cement surface.

This study found that 25% cement replacement by hydrogel microcapsules and the nanoclays did not significantly impact either measurement or result in any mortality of the coral. Hence, it can be concluded that cement replacement with metakaolin and hydrogel microcapsules had no negative impact on coral health and attachment and can therefore be considered a valid cement replacement for artificial coral reefs. The findings can have substantial implications in the regions where coral reefs are the most vulnerable, particularly in tropical South East Asia.

Moreover, the potential of geopolymers based on sustainably-sourced nanoclays such as kaolin and halloysite, biomineralized CaCO<sub>3</sub>, hydrogels, and pozzolanic nanoclays as artificial coral reef materials can be elucidated from the findings of this study. Future research is needed to more clearly ascertain the influence of these constituents on coral health and attachment, and to assess the durability of artificial coral reefs composed of such materials.

## Conflicts of interest

There are no conflicts to declare.

## Notes and references

- N. Knowlton, R. E. Brainard, R. Fisher, M. Moews, L. Plaisance and M. J. Caley, in *Life in the World's Oceans: Diversity, Distribution and Abundance*, 2010.
- G. J. Williams, N. A. J. Graham, J. B. Jouffray, A. V. Norström, M. Nyström, J. M. Gove, A. Heenan and L. M. Wedding, *Funct. Ecol.*, 2019, **33**(6), 1014–1022.
- L. Burke, K. Reytar, M. Spalding and A. Perry, *Reefs at Risk Revisited*, 2011.
- L. Boström-Einarsson, R. C. Babcock, E. Bayraktarov, D. Ceccarelli, N. Cook, S. C. A. Ferse, B. Hancock, P. Harrison, M. Hein, E. Shaver, A. Smith, D. Suggett, P. J. Stewart-Sinclair, T. Vardi and I. M. McLeod, *PLoS One*, 2020, **15**(1), e0226631.
- P. L. Choo, S. Magupin, M. A. Syed Hussein, Z. Waheed and A. Yang Amri, in *The Marine Ecosystems of Sabah*, Penerbit Universiti Malaysia Sabah, 2022, pp. 173–187.
- Jabatan Taman Laut Malaysia, *Total Economic Value of Marine Biodiversity*, 2015.
- M. Safuan, H. B. Wee, Y. S. Ibrahim, I. Idris and Z. Bachok, *J. Sustain. Sci. Manag.*, 2016, 108.
- O. Hoegh-Guldberg, E. S. Poloczanska, W. Skirving and S. Dove, *Front. Mar. Sci.*, 2017, **4**(158), DOI: [10.3389/fmars.2017.00158](https://doi.org/10.3389/fmars.2017.00158).
- T. P. Hughes, J. T. Kerry, A. H. Baird, S. R. Connolly, A. Dietzel, C. M. Eakin, S. F. Heron, A. S. Hoey, M. O. Hoogenboom, G. Liu, M. J. McWilliam, R. J. Pears, M. S. Pratchett, W. J. Skirving, J. S. Stella and G. Torda, *Nature*, 2018, **556**, 492–496.
- A. J. Edwards, J. Guest, S. Shafir, D. Fisk, E. Gomez, B. Rinkevich, A. Heyward, M. Omori, K. Iwao, R. Dizon, A. Morse, C. Boch, S. Job, L. Bongiorno, G. Levy, L. Shaish and S. Wells, *Reef Rehabilitation Manual*, 2010.
- A. N. Umar, R. Anwar, O. H. Hassan and Z. Zakaria, in *Proceedings of the International Symposium on Research of Arts, Design and Humanities (ISRADH 2014)*, 2015.
- A. R. bin Latun and M. P. bin Abdullah, *Pap. Present. Symp. Artif. Reefs Fish Aggregating Devices as Tools Manag. Enhanc. Mar. Fish. Resour.*, Colombo, Sri Lanka, 1990.
- E. Higgins, A. Metaxas and R. E. Scheibling, *PLoS One*, 2022, 17.
- L. Harrington, K. Fabricius, G. De'Ath and A. Negri, *Ecology*, 2004, **85**, 3428–3437.
- T. J. Goreau, *Nat. Resour.*, 2014, **5**, 527–537.
- M. G. Sabater and H. T. Yap, *J. Exp. Mar. Biol. Ecol.*, 2002, **272**, 131–146.
- S. M. Strömberg, T. Lundälv and T. J. Goreau, *J. Exp. Mar. Biol. Ecol.*, 2010, **395**, 153–161.
- M. Fahimzadeh, P. Pasbakhsh, L. S. Mae, J. B. L. Tan and R. K. S. Raman, *Engineering*, 2022, **13**, 217–237.
- A. Røyne, Y. J. Phua, S. Balzer Le, I. G. Eikjeland, K. D. Josefsen, S. Markussen, A. Myhr, H. Throne-Holst, P. Sikorski and A. Wentzel, *PLoS One*, 2019, **14**, e0212990.
- V. Wiktor and H. M. Jonkers, *Smart Mater. Struct.*, 2016, **25**, 84006.
- V. Wiktor and H. M. Jonkers, *Cem. Concr. Compos.*, 2011, **33**, 763–770.
- M. Fahimzadeh, P. Pasbakhsh, L. S. Mae, J. B. L. Tan and R. K. S. Raman, *Appl. Clay Sci.*, 2023, **240**, 106979.
- W. Khaliq and M. B. Ehsan, *Constr. Build. Mater.*, 2016, **102**, 349–357.
- M. Fahimzadeh, A. D. Abeyratne, L. S. Mae, R. K. Raman Singh and P. Pasbakhsh, *Materials*, 2020, **13**, 3711.
- V. W. Wiktor and H. M. Jonkers, *Smart Mater. Struct.*, 2016, **25**, 84008.
- L. Liu, Y. Wan, Y. Xie, R. Zhai, B. Zhang and J. Liu, *Chem. Eng. J.*, 2012, **187**, 210–216.
- Y. Jin, R. Yendluri, B. Chen, J. Wang and Y. Lvov, *J. Colloid Interface Sci.*, 2016, **466**, 254–260.
- T. Yu, B. Zhang, P. Yuan, H. Guo, D. Liu, J. Chen, H. Liu and L. Setti Belaroui, *Constr. Build. Mater.*, 2023, **389**, 131709.
- T. T. Haw, F. Hart, A. Rashidi and P. Pasbakhsh, *Appl. Clay Sci.*, 2020, **188**, 105533.
- B. Zhang, H. Guo, P. Yuan, Y. Li, Q. Wang, L. Deng and D. Liu, *Appl. Clay Sci.*, 2020, **185**, 105375.
- M. Li, X. Zhu, A. Mukherjee, M. Huang and V. Achal, *J. Hazard. Mater.*, 2017, **329**, 178–184.



- 32 B. Zhang, T. Yu, H. Guo, J. Chen, Y. Liu and P. Yuan, *Clays Clay Miner.*, 2022, **70**, 882–902.
- 33 J. Li, Q. Yang, J. Dong, M. Sweet, Y. Zhang, C. Liu, Y. Zhang, X. Tang, W. Zhang and S. Zhang, *Engineering*, 2022, **28**, 105–116.
- 34 S. Hollanders, R. Adriaens, J. Skibsted, Ö. Cizer and J. Elsen, *Appl. Clay Sci.*, 2016, **132**, 552–560.
- 35 K. S. Singh and S. G. Sawant, *Indian J. Geo-Marine Sci.*, 2022, **51**.
- 36 T. Zhao, X. Han, L. He, Y. Jia and R. C. Yu, *ACS Omega*, 2023, **8**, 702–708.

